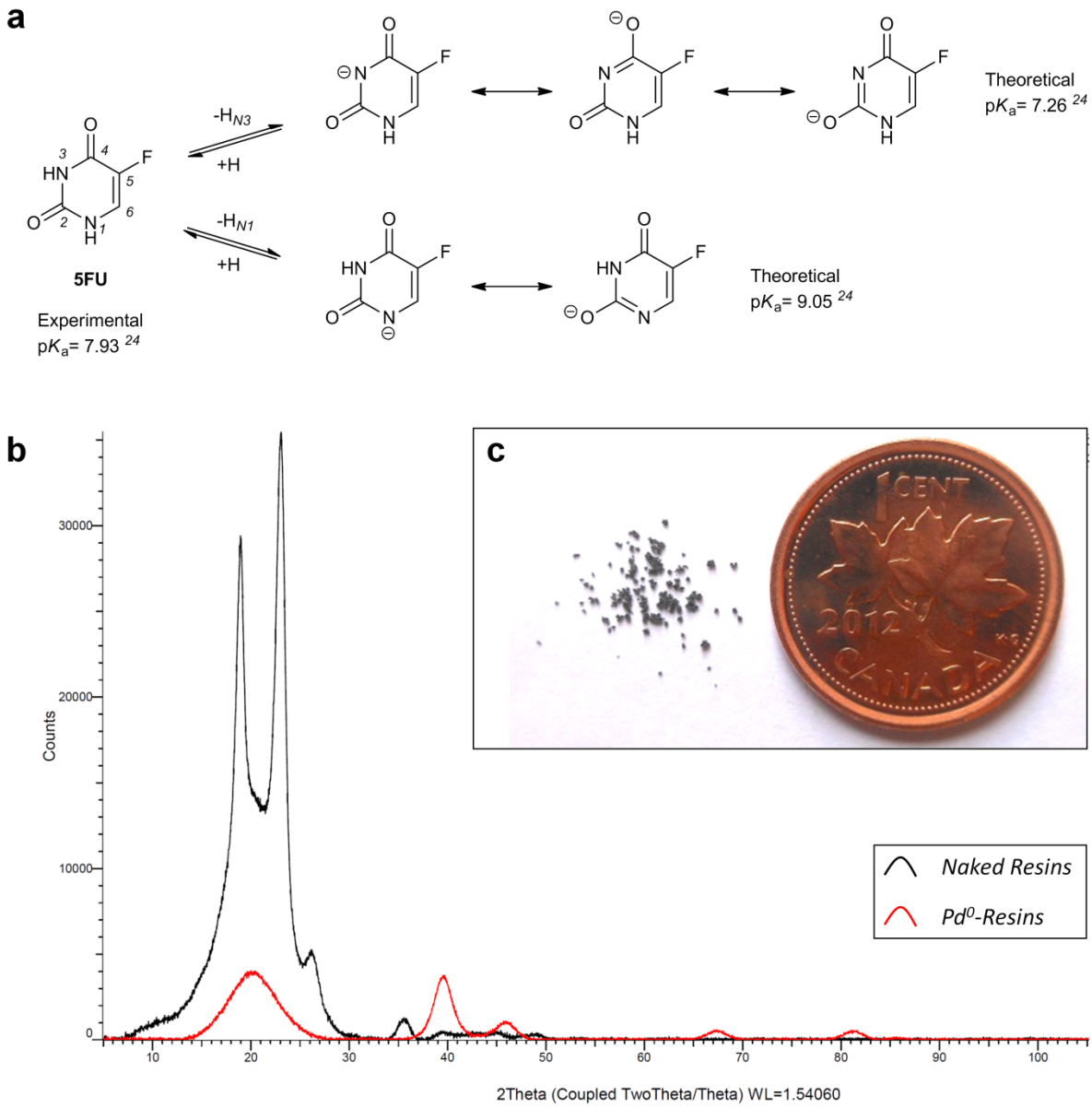

Supplementary Figure 1 | (**a**) 5FU and its conjugate bases: Effect on pK_a. The low experimental pK_a of 5FU is in part due to the delocalization of the resulting negative charge across the π system. (**b**) X-ray diffraction spectra of non-functionalized commercial NovaSyn TG amino HL resins (**naked resins**, in black) compared to Pd^0-functionalized resins (**Pd^0-resins**, in red). Both samples showed the semi-amorphous structure of the PEG-polystyrene matrix at 20 degrees, while the distinctive pattern of crystalline Pd^0 was only observed in the **Pd^0-resins** spectra as 4 peaks between 40 and 82 degrees. (**c**) Image of **Pd^0-resins** next to 1 Canadian cent (19.05 mm in diameter).

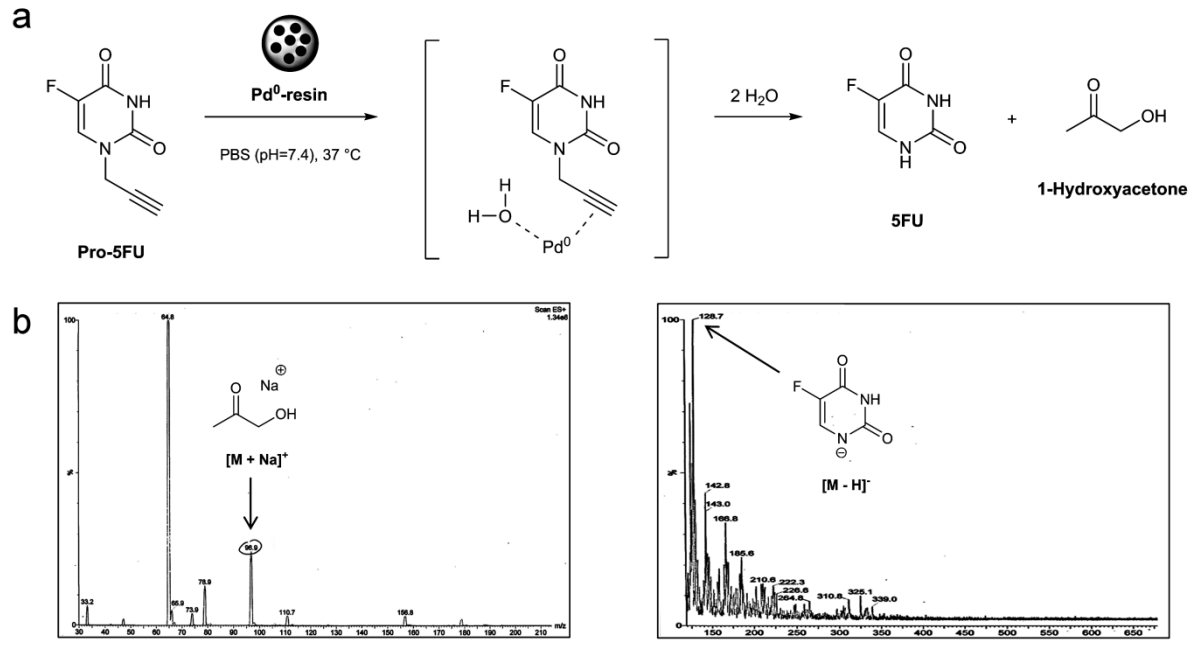

Supplementary Figure 2 | (**a**) Pd^0-mediated conversion of **Pro-5FU** into **5FU** and 1-hydroxyacetone in aqueous media (allenyl-palladium (II) intermediate not represented). (**b**) Low resolution mass spec (Electrospray ionization (ES)) analysis of reaction crude after reaction completion (monitored by HPLC). Left panel ES- showing **1-hydroxyacetone** $[M + Na]^+$ peak; right panel, ES+ showing **5FU** $[M - H]^-$ peak.

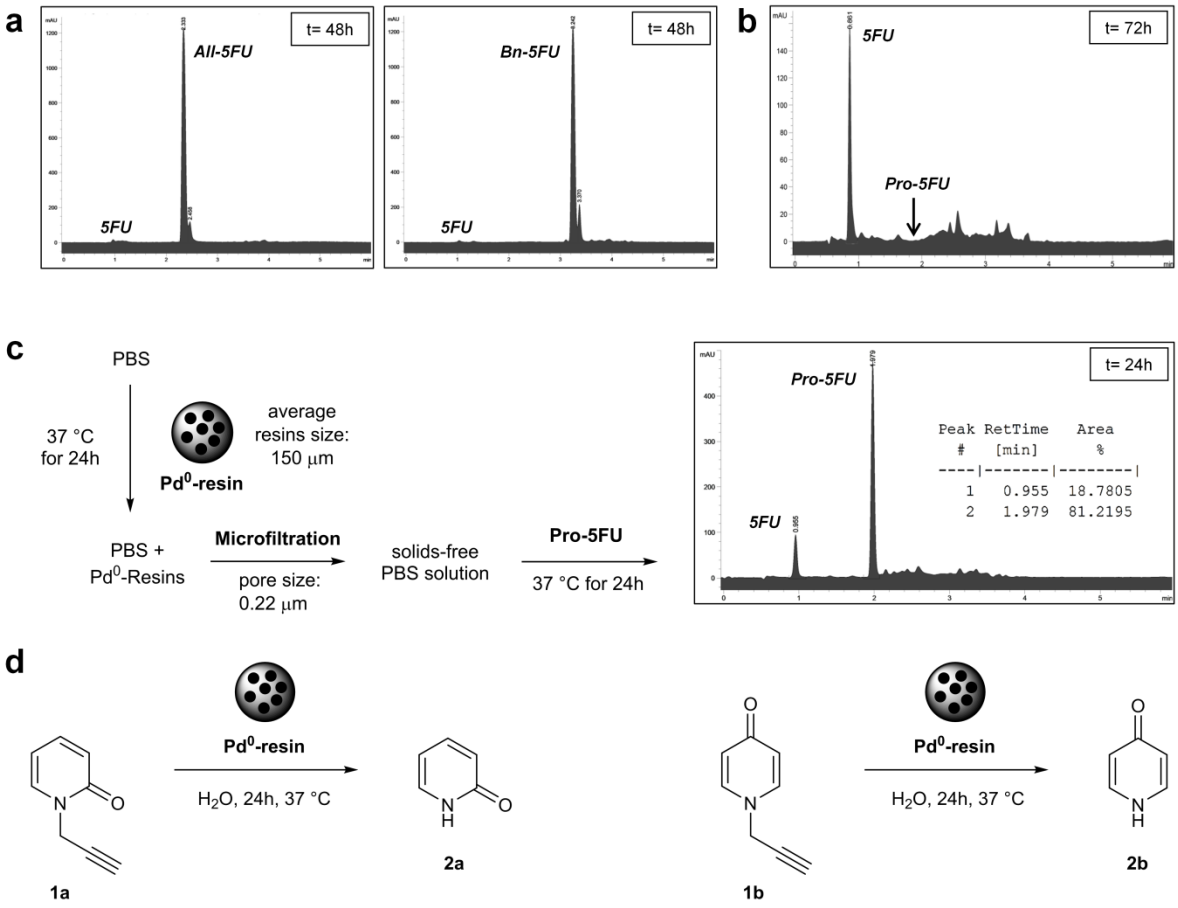

Supplementary Figure 3 | (**a**) Treatment of **All-5FU** and **Bn-5FU** with **Pd^0-resins**. **Pd^0-resins** (1 mg / mL, [Pd^0] ~ 266 μM) were dispersed into a solution of **All-5FU** or **Bn-5FU** (100 μM) in 0.1% (v/v) DMSO in PBS and incubated for 48h at 37 °C. Reaction crude was monitored by HPLC using the UV detector at 280nm: left panel, **All-5FU** experiment; right panel, **Bn-5FU** experiment. (**b**) Treatment of **Pro-5FU** with sub-stoichiometric amounts of **Pd^0-resins**. **Pd^0-resins** (1 mg / mL, [Pd^0] ~ 266 μM) were dispersed into a solution of **Pro-5FU** (300 μM) in 0.1% (v/v) DMSO in PBS, incubated for 72h at 37 °C and analyzed by HPLC. (**c**) Heterogeneous catalysis study. **Pd^0-resins** (2 mg) were dispersed into a PBS solution (2 mL) and incubated for 24h at 37 °C. The mixture was filtrated using a Millipore microfilter (0.22 μm) and, subsequently, **Pro-5FU** added to the mixture (final concentration= 100 μM). The reaction mixture was incubated for additional 24 h and analyzed by HPLC (UV detector at 280nm). (**d**) Pd^0-mediated depropargylation of **1-propargyl-2-pyridone** (**1a**) and **1-propargyl-4-pyridone** (**1b**). **Pd^0-resins** (1 mg / mL, [Pd^0] ~ 266 μM) were dispersed into a solution of compounds **1a** or **1b** (100 μM) in 0.1% (v/v) DMSO in PBS and incubated at 37 °C. After 24h, TLC showed no traces of starting material and the formation of deprotected compounds **2a,b**.

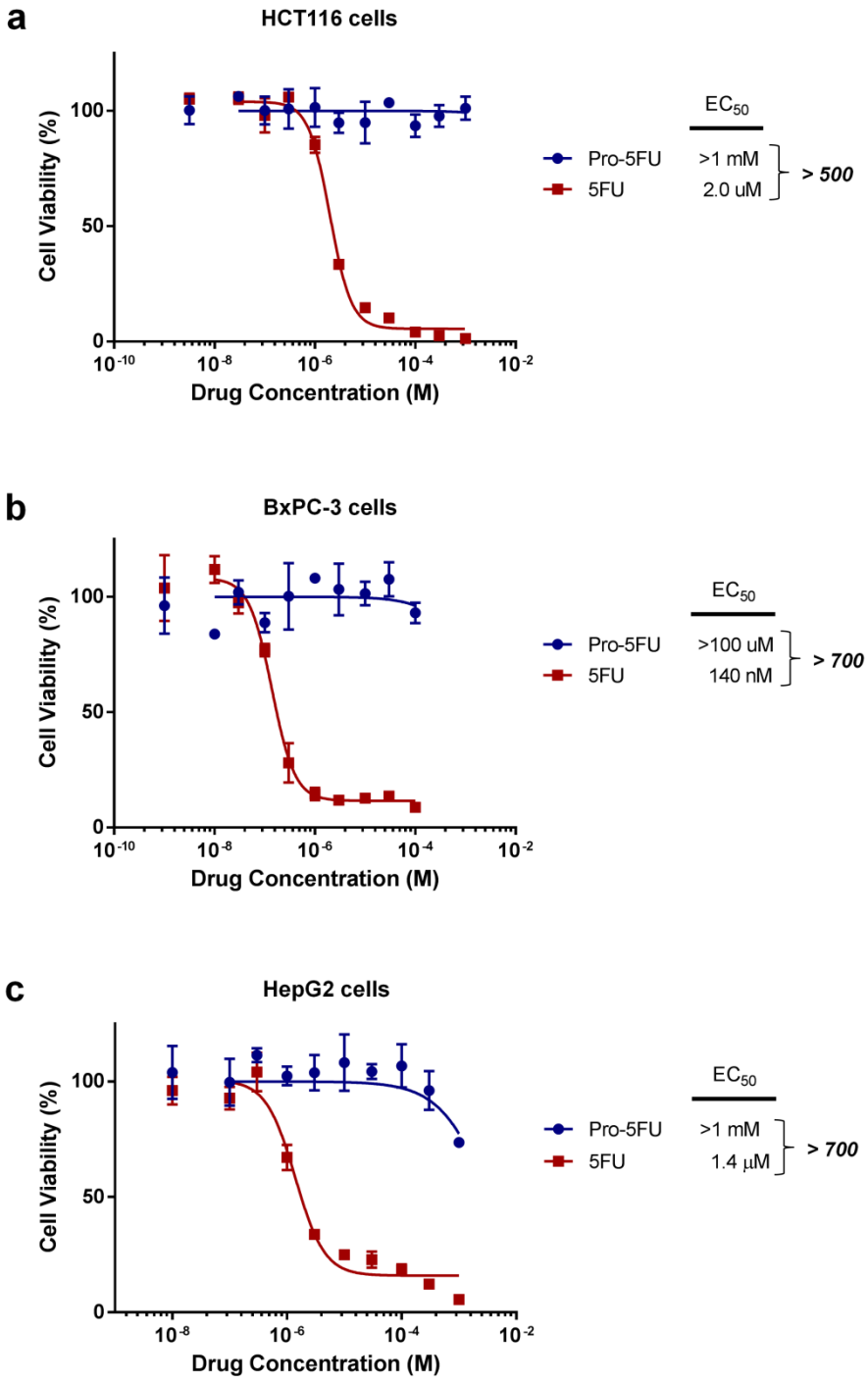

Supplementary Figure 4 | Study of Pro-5FU bioorthogonality. Cytotoxic effect of **Pro-5FU** in comparison to unmodified **5FU**. Cells were incubated with increasing concentrations of **Pro-5FU** and **5FU** (0.01-1,000 µM) for 5 days and cell viability measured (PrestoBlue™ assay) to determine the corresponding EC_{50} values. (**a**) colorectal HCT116 cancer cells. (**b**) pancreatic BxPC-3 cancer cells. (**c**) liver HepG2 cancer cells.

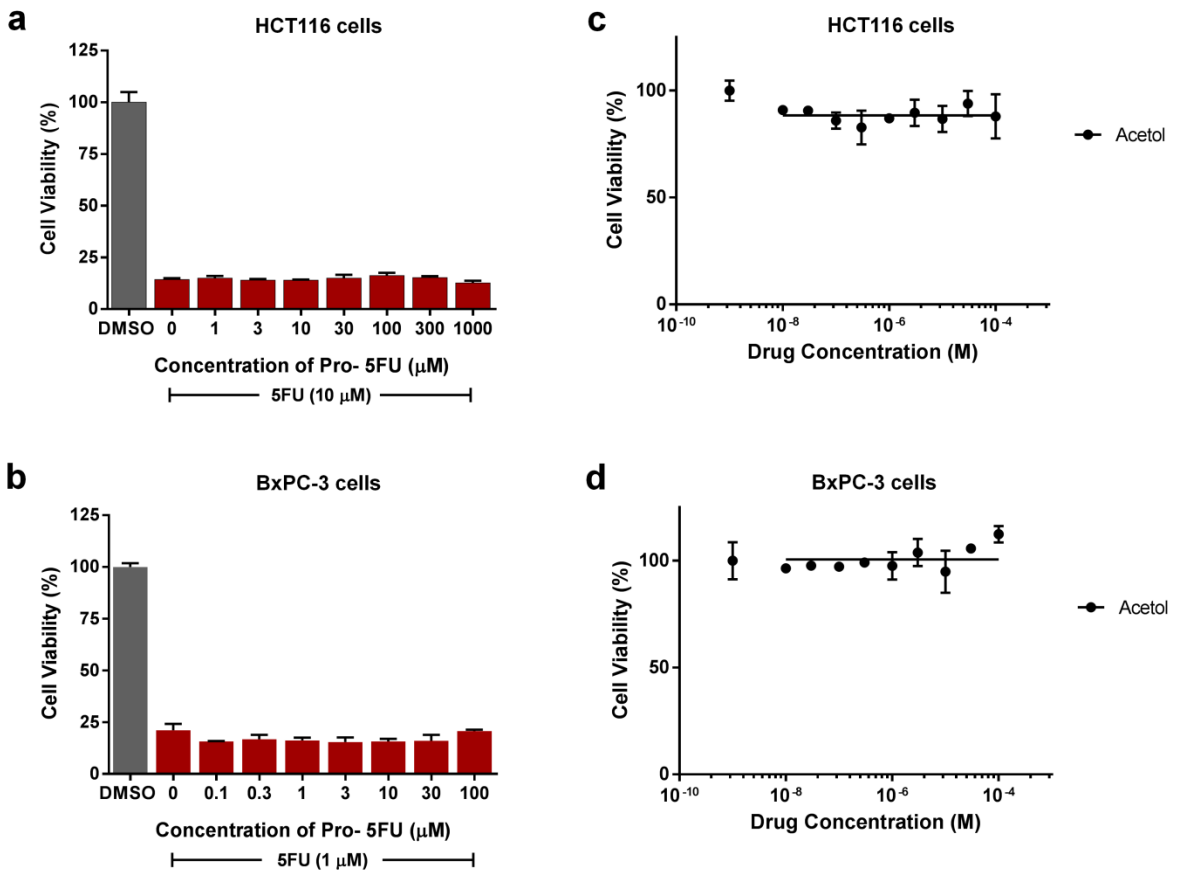

Supplementary Figure 5 | (**a-b**) Study of pharmacological interactions between **5FU** and **Pro-5FU**. Cells were incubated with **5FU** (10 µM for HCT116 cells and 1 µM for BxPC-3 cells) in combination with increasing concentrations of **Pro-5FU** (0.1-1,000 µM), and cell viability determined. (**c-d**) Study of cytotoxicity of 1-hydroxyacetone (acetol) in HCT116 and BxPC-3 cells. Cells were incubated with increasing concentrations of acetol (0.01-100 µM) for 5 days and cell viability measured (PrestoBlue™ assay).

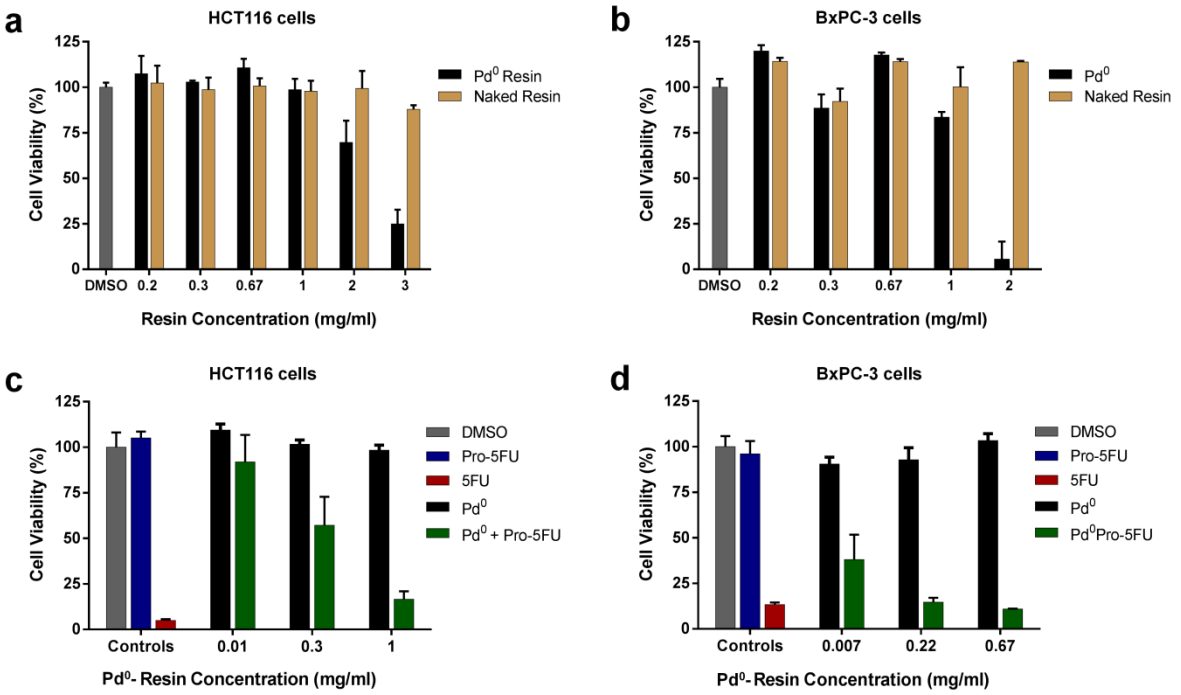

Supplementary Figure 6 | Bioorthogonality and catalytic study of Pd^0-resins. (**a-b**) Study of unspecific cytotoxic effect induced by **Pd^0-resins**. Increasing quantities of **Pd^0-resins** and (non-functionalized) **naked resins** (0.1-3 mg / mL) were incubated with cells for 5 days and cell viability determined by PrestoBlue™ assay. (**c-d**) Determination of optimal **Pd^0-resin** concentration (0.1-1 mg / mL) to generate pharmacologically active levels of drug via **Pro-5FU** dealkylation. [**Pro-5FU**] = [**5FU**] = 100 µM for HCT116 cells and 30 µM for BxPC cells. (**a,c**) colorectal HCT116 cells; (**b,d**) pancreatic BxPC-3 cells.

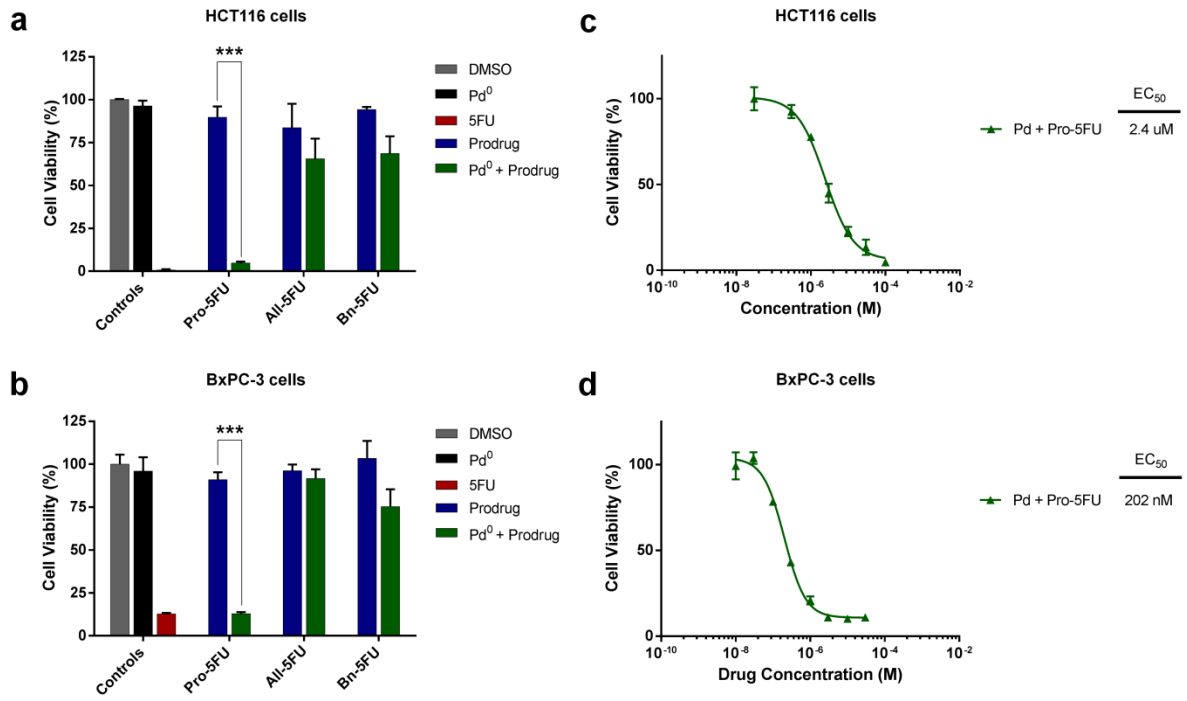

Supplementary Figure 7 | (**a,b**) Preliminary BOOM conversion study with **5FU** prodrugs. Experiments: 0.1% (v/v) DMSO in media (untreated cell control); 1 or 0.66 mg / mL of **Pd^0-resins** (negative control); prodrug (100 µM for HCT116 cells and 30 µM for BxPC-3 cells; negative control); and **Pd^0-resins** (1 or 0.66 mg / mL) + prodrug (100 µM for HCT116 cells and 30 µM for BxPC-3 cells; BOOM conversion assay). Following 5 days of treatment, cell viability (PrestoBlue™ assay) was determined and compared to analyze significant effects. *** $p < 0.001$ (n=3). (**c-d**) Dose response study of **Pd^0-resins** + **Pro-5FU** combinations. Cells were incubated with **Pd^0-resins** (1 mg / mL for HCT116 cells and 0.66 mg / mL for BxPC-3 cells) plus increasing concentrations of **Pro-5FU** (0.01-1,000 µM) for 5 days and cell viability measured (PrestoBlue™ assay) to determine the corresponding EC_{50} values. (**a,c**) colorectal HCT116 cells; (**b,d**) pancreatic BxPC-3 cells.

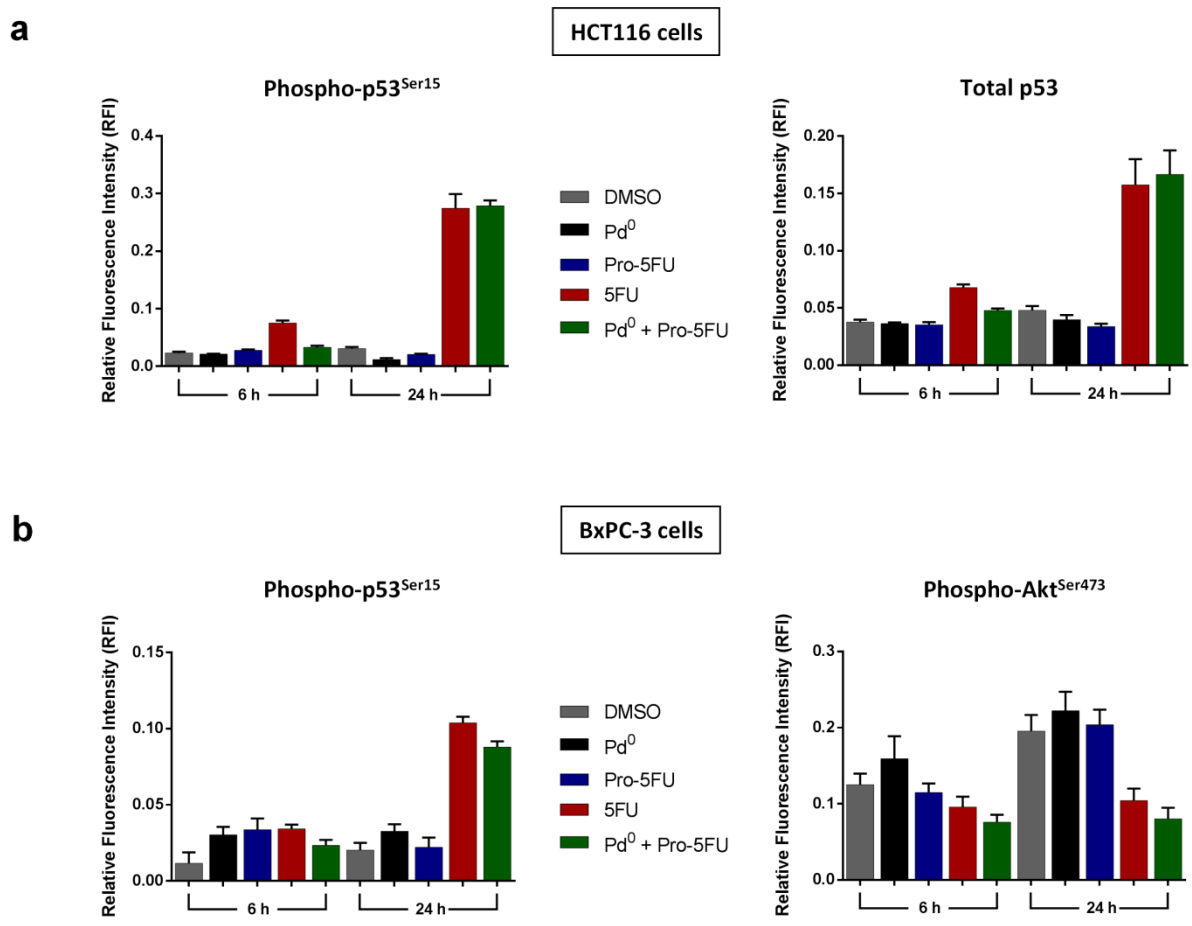

Supplementary Figure 8 | Significant phenotypic modifications identified from Zeptosens Reverse Protein Microarray analysis in colorectal HCT116 cells (**a**) and BxPC-3 cells (**b**). Bar graphs represent the median relative fluorescence intensity (RFI) values and standard deviation calculated across a 4-fold protein concentration series extracted from each sample. Data represents the relative abundance of phosphorylated p53 (left) and total p53 protein / phosphorylated Akt (right) across negative control samples (untreated cells, **Pd^0-resins** and **Pro-5FU**), positive control sample (**5FU**) and **Pd^0–resins** + **Pro-5FU** combination sample at 6 and 24 h treatment exposures.

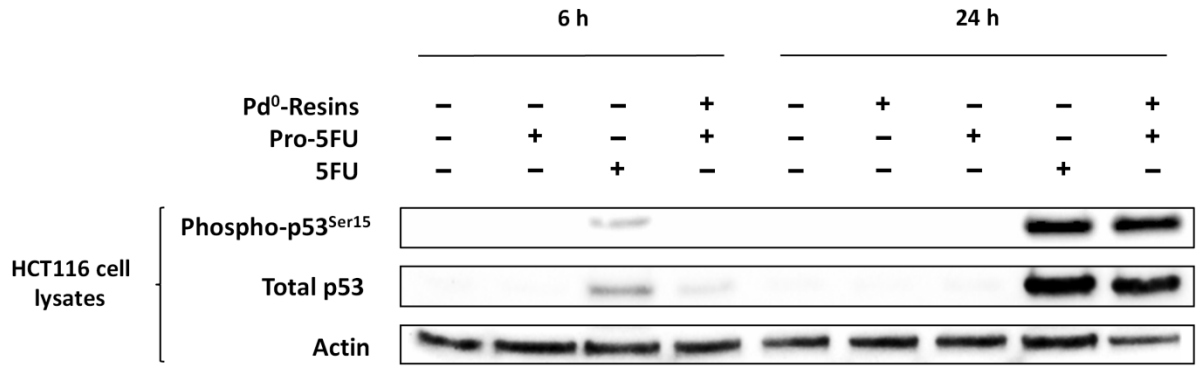

Supplementary Figure 9 | Western Blot analysis of total p53 and phosphorylated p53 in colorectal HCT116 cells across different exposure times (6 and 24 h) and treatments: negative controls (untreated cells, **Pd^0-resins** and **Pro-5FU**), positive control (**5FU**) and **Pd^0-resins** + **Pro-5FU** (BOOM conversion assay).

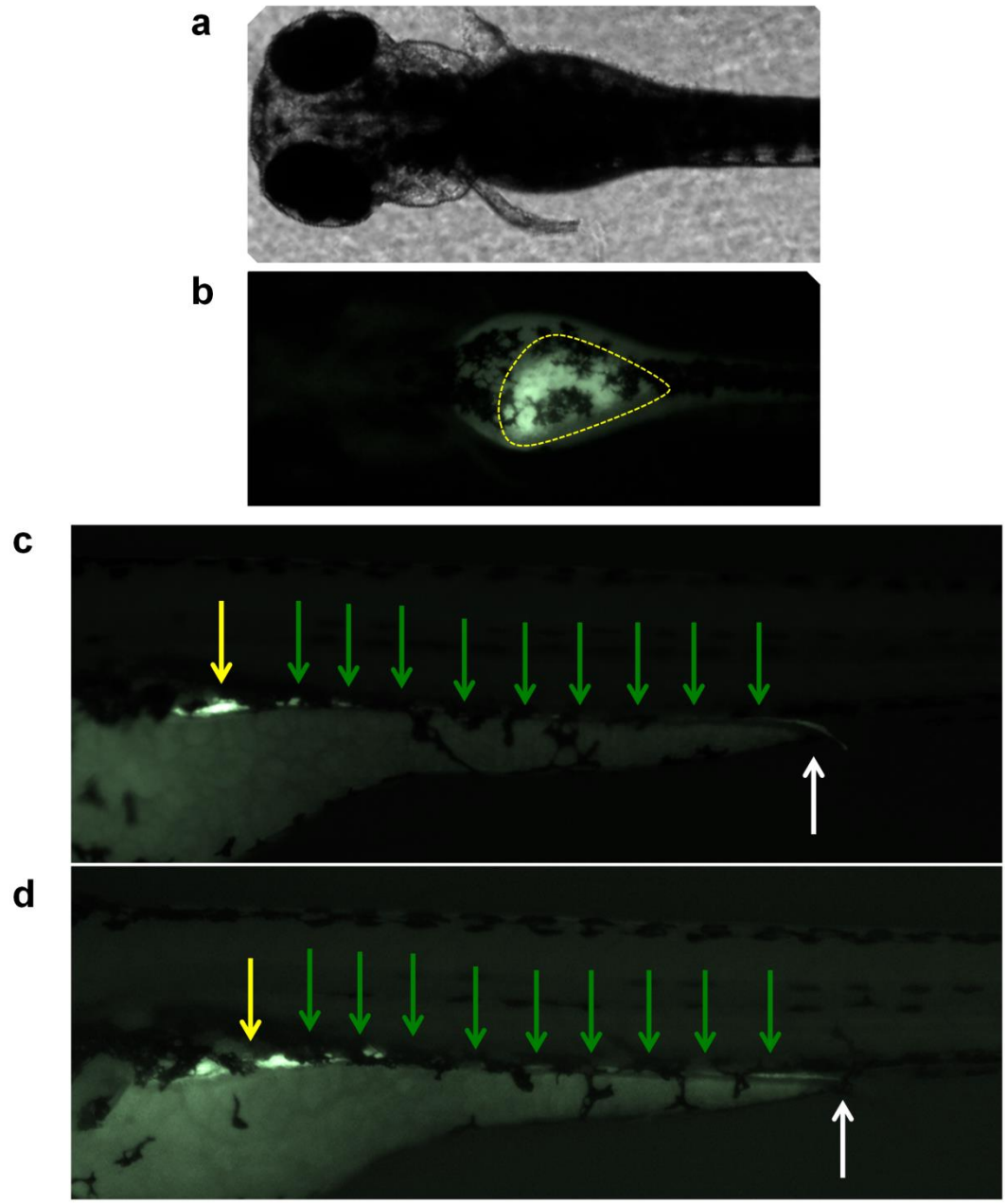

Supplementary Figure 10 | Bioactivation of compound **3** in zebrafish embryos. Zebrafish embryos (3dpf, n=5) were incubated with compound **3** (5 µM) for 24 h at 28.5 °C and imaged using fluorescent microscopy (Ex / Em: 488 / 521 nm). (**a**,**b**) Ventral view of a 4dpf zebrafish embryo, in (**a**) brightfield or (**b**) with the fluorescent signal from the developing intestinal bulb outlined (yellow dashed line, possibly including the exocrine pancreas). (**c**,**d**) Lateral view of two individual zebrafish embryo showing the fluorescent signal from the developing intestinal bulb (yellow arrow), along the intestinal tract (green arrows) to the anus (white arrow).

Supplementary Table 1. Library of 30 primary antibodies used for Zeptosens reverse phase protein microarray analysis.

4E-BP1 P Ser65	Bcl-2	Bcl-x
4E-BP1 P Thr37,Thr46	Caspase 3 cleaved	β-Catenin P Ser33,Ser37,Thr41
ATM	Cyclin D1 P Thr286	ATM/ATR Substrate P Ser/Thr
Bad P Ser136	p38 MAPK	Prohibitin
Bak	p38 MAPK PThr180,Tyr182	p53
beta-Catenin P Thr41,Ser45	p53 P Ser15	GSK-3-alpha/beta P Ser21/Ser9
GSK 3 B	PARP cleaved Asp214	Akt P Ser473
NFkB p65 Ser536	Bax	XIAP
Akt	NFkB p105/p50	Histone H2A.X P Ser139
Bad P Ser112	p21 CIP/WAF1 p Thr145	Cyclin D1

SUPPLEMENTARY METHODS

Synthesis and Characterization of *N*-Propargylated Compounds 1a,b.

***N*-Propargyl-2-pyridone (1a)**.[1] 2-pyridone (**2a**) (170 mg, 1.8 mmol) was dissolved in dry DCM (4 ml) containing DBU (401 µl, 2.7 mmol). Propargyl bromide (231 µl, 2.2 mmol) was added dropwise to the mixture and the reaction stirred at room temperature overnight. The solvents were then removed *in vacuo*, the crude dissolved with EtOAc (20 ml) and washed with H_2O (20 ml). The aqueous layer was then washed twice more with EtOAc (20 ml each). The combined organic layers were then washed with brine (60 ml x 2), dried over anhydrous $MgSO_4$, the solids filtered off and concentrated *in vacuo.* The crude was purified via flash chromatography (EtOAc 2:1 Hexane), which yielded a yellow oil, 123 mg (71 % yield).

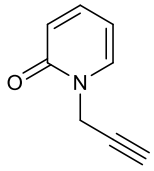

1a

Rf 0.2 (EtOAc 2:1 Hexane). ^{1}H NMR (500 MHz, $CDCl_3$) δ 7.61 (dd, *J* = 6.9, 1.9, 1H, Ar*H*), 7.32 (ddd, *J* = 8.8 Hz, 6.6, 2.0, 1H, Ar*H*), 6.54 (d, *J* = 9.2 Hz, 1H, Ar*H*), 6.22 (td, *J* = 6.8 Hz, 1.2, 1H, Ar*H*), 4.73 (d, *J* = 2.6 Hz, 2H, N–C*H*$_2$–C), 2.47 (t, *J* = 2.6 Hz, 1H, C≡C*H*). ^{13}C NMR (126 MHz, $CDCl_3$) δ 162.10 (C), 139.91 (CH), 135.93 (CH), 120.69 (CH), 106.48 (CH), 76.99 (C), 75.47 (CH), 37.71 (CH_2). MS (ESI) (*m/z*) 134.2 $(M+H)^+$.

***N*-Propargyl-4-pyridone (1b)**.[2] 4-pyridone (**2b**) (300 mg, 3.2 mmol) was dissolved in dry DCM (4 ml) containing DBU (1415 µl, 9.5 mmol) and the reaction mixture cooled to 4 °C. Afterwards, propargyl bromide (674 µl, 6.3 mmol) was added dropwise and the reaction stirred at room temperature for 2 h. The solvents were then removed *in vacuo*, the crude dissolved in isopropanol : $CHCl_3$ (1:3, 40 ml) and washed with ddH_2O (40 ml). The aqueous layer was then washed four times more with $CHCl_3$ (40 ml). The combined organic layers were then washed with brine (200 ml x 2), dried over anhydrous $MgSO_4$, the solids filtered off and concentrated *in vacuo.* The crude was purified via flash chromatography (8 % MeOH in DCM) to yield pure compound **1b** as a colourless oil (104 mg, 25 %).

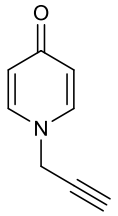

1b

Rf 0.4 (10% MeOH in DCM). ^{1}H NMR (500 MHz, $CDCl_3$) δ 7.45 – 7.36 (m, 2H, Ar*H*), 6.41 – 6.31 (m, 2H, Ar*H*), 4.57 (d, *J* = 2.6 Hz, 2H, N–CH_2–C), 2.62 (t, *J* = 2.6 Hz, 1H, C≡C*H*). ^{13}C NMR (126 MHz, $CDCl_3$) δ 179.06 (C), 139.22 (CH), 119.03 (CH), 77.13 (C), 75.45 (CH), 45.50 (CH_2). MS (ESI) (*m/z*) 134.2 $(M+H)^+$.

Supplementary References

1. F. Mohr, A. Mendía & M. Laguna. Platinum(II) alkynyl complexes containing N- and S-propargylated ligands: synthesis, structures and formation of Pt^{II}/Ag^{I} coordination compounds. *Eur. J. Inorg. Chem.* **19**, 3115-3123 (2007).

2. C. Aubert, P. Betschmann, M. J. Eichberg, V. Gandon, T. J. Heckrodt, J. Lehmann, M. Malacria, B. Masjost, E. Paredes, K. Vollhardt, C. Peter & G. D. Whitener. Cobalt-mediated [2 + 2 + 2] cycloaddition versus C-H and N-H activation of pyridones and pyrazinones with alkynes: an experimental study. *Chem. Eur J.* **13**, 7443-7465 (2007).